SURE 静岡大学学術リポジトリ
Shizuoka University REpository

SOI metal-oxide-semiconductor field-effect transistor photon detector based on single-hole counting

メタデータ	言語: eng 出版者: 公開日: 2011-10-06 キーワード (Ja): キーワード (En): 作成者: Du, Wei, Inokawa, Hiroshi, Satoh, Hiroaki, Ono, Atsushi メールアドレス: 所属:
URL	http://hdl.handle.net/10297/6183

SOI metal-oxide-semiconductor field-effect transistor photon detector based on single-hole counting

Wei Du,* Hiroshi Inokawa, Hiroaki Satoh, and Atsushi Ono

Research Institute of Electronics, Shizuoka University, Hamamatsu 432-8011, Japan
*Corresponding author: duwei@rie.shizuoka.ac.jp

Received February 25, 2011; revised June 21, 2011; accepted June 23, 2011;
posted June 24, 2011 (Doc. ID 143208); published July 20, 2011

In this Letter, a scaled-down silicon-on-insulator (SOI) metal-oxide-semiconductor field-effect transistor (MOSFET) is characterized as a photon detector, where photogenerated individual holes are trapped below the negatively biased gate and modulate stepwise the electron current flowing in the bottom channel induced by the positive substrate bias. The output waveforms exhibit clear separation of current levels corresponding to different numbers of trapped holes. Considering this capability of single-hole counting, a small dark count of less than $0.02\,s^{-1}$ at room temperature, and low operation voltage of 1 V, SOI MOSFET could be a unique photon-number-resolving detector if the small quantum efficiency were improved. © 2011 Optical Society of America

OCIS codes: 040.5160, 040.3780, 040.6040, 040.6070, 230.5160.

Single-photon detectors attract much attention due to their variety of applications, such as in fluorescence lifetime measurement [1], DNA microarrays [2], and quantum cryptography [3]. However, conventional single-photon detectors, i.e., photomultiplier tubes (PMTs) and avalanche photodiodes (APDs), rely on carrier multiplication and still have some issues in terms of dark counts, operation speed limited by the recovery time and after pulses, high operation voltage, etc. [4]. Since these issues stem mainly from the carrier multiplication by a high electric field, improvement can be achieved by directly detecting photogenerated carriers one by one without any multiplication. Such detectors [5–7] are expected to have photon number resolution (PNR), which is useful in some classes of quantum key distribution [8] and quantum computation [9]. Although PNR can be attained by PMTs [10] or APDs [11], the resolution is limited. Detectors such as transition edge sensors [12], visible light photon counters [13], and parallel nanowire detectors [14] have better resolution, but operate only at cryogenic temperatures.

It has been reported that a short- and narrow-channel silicon-on-insulator (SOI) metal-oxide-semiconductor field-effect transistor (MOSFET) could operate at room temperature as a photon detector based on single-carrier counting [6,7]. It detected photogenerated carriers one by one without multiplication, and features a very low dark count and small operation voltage. However, the counting rate of the detector was less than $10\,s^{-1}$, and spectroscopic response and pulse counting statistics were not known. In this Letter, we further pursue the possibility of this type of photon detector using a scaled-down (65 nm gate length L and 105 nm channel width W) SOI MOSFET.

Figure 1 shows (a) the top and (b) cross-sectional views of the device [15,16]. In this structure, photogenerated holes can be trapped under the lower gate (LG) when negative voltage ($V_{LG} < 0$) is applied, whereas the back electron channel, which is used as an electrometer, can be formed with positive substrate voltage ($V_{SUB} > 0$) [6]. Photogeneration of holes and their recombination will modulate the electron current and can be detected as pulses.

Figure 2 shows drain current waveforms for different levels of incident light intensity at a wavelength of 550 nm at 300 K. We shift each waveform for clarity. It shows that the pulse count increases as the light intensity increases. Moreover, different pulse levels can be seen clearly, suggesting that a different number of holes is trapped under the LG. The first, second, third, and fourth levels correspond to zero, one, two, and three trapped holes, respectively. Note that the dark counts are less than $0.02\,s^{-1}$ (two counts in 110 s). The bias voltages are less than or equal to 1 V, much less than those of PMTs and APDs.

There is proportionality between pulse count rate and nominal photon incident rate, as shown in Fig. 3. Here, the number of rising edges in the waveform was counted,

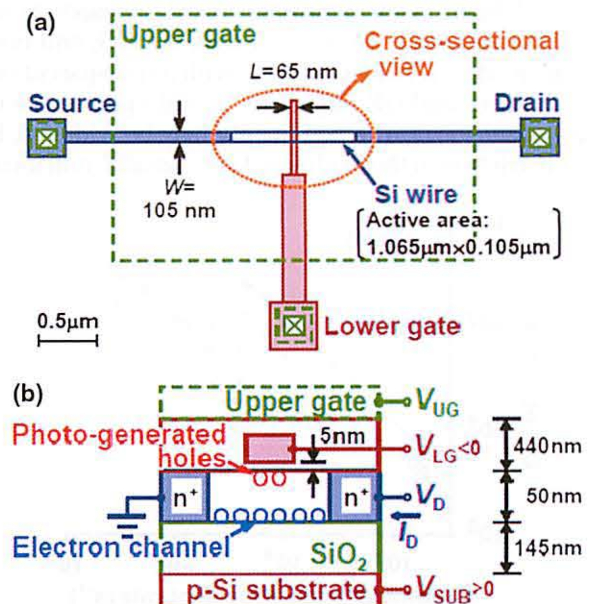

Fig. 1. (Color online) Device structure. (a) Top view. (b) Cross-sectional view. The thicknesses of the buried oxide, SOI, LG oxide, and insulator below the UG) are 145, 50, 5, and 440 nm, respectively.

0146-9592/11/152800-03$15.00/0 © 2011 Optical Society of America

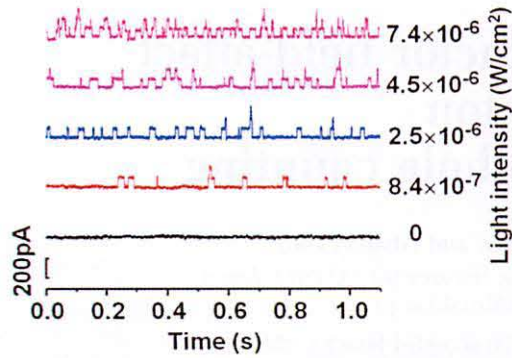

Fig. 2. (Color online) Drain current waveforms at 300 K for different levels of light intensity at a wavelength of 550 nm. Base line current is about 1 nA, and each waveform is shifted for clarity. V_D, V_{LG}, V_{UG}, and V_{SUB} are 0.05, −1, −0.6, and 1 V, respectively.

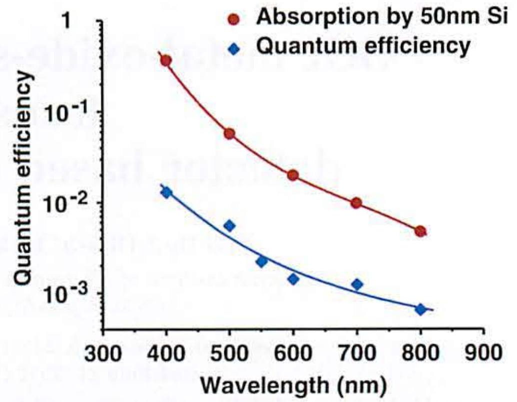

Fig. 4. (Color online) Nominal quantum efficiency with respect to the wavelength. Light absorption by the 50 nm Si slab calculated from the absorption coefficient is also shown.

and the nominal photon incident rate was obtained by multiplying the light intensity and the active area shown in Fig. 1(a). Nominal quantum efficiency (QE) can be obtained from the proportionality constant and is plotted in Fig. 4 as a function of wavelength. Light absorption by a 50 nm thick Si slab is nearly parallel to the experimental data, indicating that the spectroscopic behavior of QE is governed mainly by the Si absorption coefficient. Although the highest QE (1.3%) at the shortest wavelength (400 nm) is rather low, the noise equivalent power (NEP) [8] is as small as $7.7 \times 10^{-18}\ \mathrm{W}/\sqrt{\mathrm{Hz}}$ owing to the small dark counts. However, the detectivity $D^* = (\text{active area})^{1/2}/\text{NEP}$ figure of merit considering the active area is only $4.3 \times 10^{12}\ \mathrm{cm}\sqrt{\mathrm{Hz}}\ \mathrm{W}^{-1}$. This value is comparable to that of an ordinary Si photodiode (for example, Hamamatsu Photonics S1336-18BK), but 2 orders of magnitude smaller than that of an APD (for example, Perkin-Elmer SPCM-AQRH-16). The low QE results from the metallic upper gate (UG) covering the entire active area of the device, i.e., the device only receives the scattered light by lines for electrical connection and probing pads on the same level with the UG, and could be improved by replacing the UG with a transparent one. Effective area and QE might also be enlarged by the use of an antenna [17]. The active area may be widened, but the constriction in the Si channel (i.e., small L and locally small W) have to be made to keep the high sensitivity to single holes, and the collection efficiency and the transit speed of the photogenerated holes may be another concern. The maximum count rate in Fig. 3 is about $300\ \mathrm{s}^{-1}$ for the amplifier (DL instruments, Model 1211) used in this measurement. Note that pulse width determined by the hole lifetime does not limit the count rate as long as the rising edges are counted.

Figures 5(a)–5(e) are histograms of drain currents corresponding to Fig. 2. The solid symbols are obtained data and the solid curves are fitting curves with Gaussian

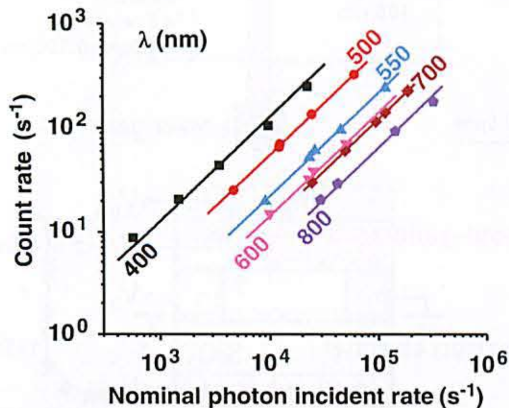

Fig. 3. (Color online) Count rate as a function of nominal photon incident rate for different wavelengths. Solid symbols are measured data and solid curves are fitted lines with a fixed slope of 1.

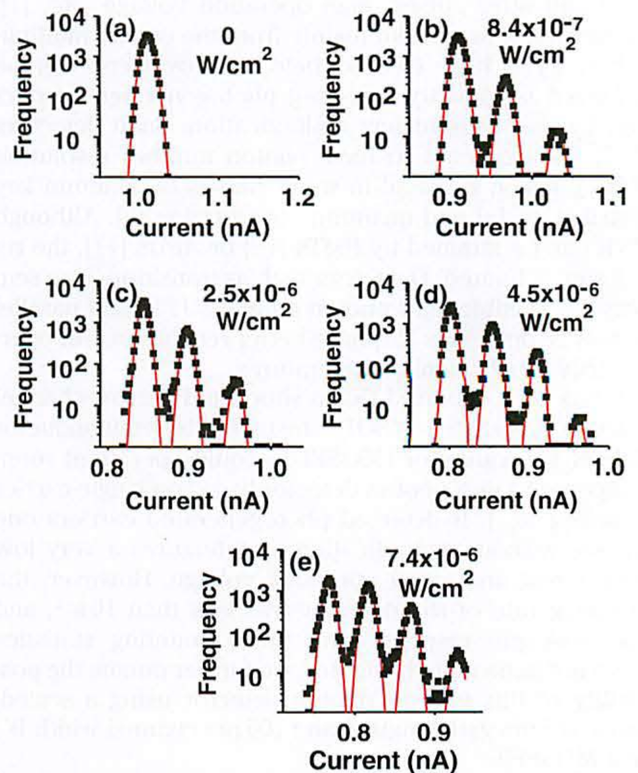

Fig. 5. (Color online) Histograms of digitized drain currents corresponding to Fig. 2. The first, second, third, and fourth peaks from left in each graph correspond to zero, one, two, and three trapped holes, respectively. Data acquisition time period and time step are 1.56 s and 61 μs, respectively, and 25,600 ($= 1.56\ \mathrm{s}/61\ \mu\mathrm{s}$) data points (current values) are classified into bins with a width of 2 pA.

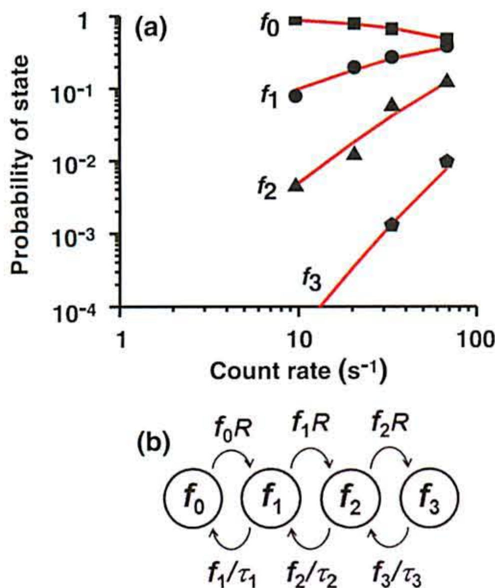

Fig. 6. (Color online) (a) Probability of states obtained from Fig. 5 as a function of count rate, namely, hole generation rate R. States f_0, f_1, f_2, and f_3 correspond to zero, one, two, and three trapped holes, respectively. (b) State transition diagram to explain (a).

distribution. The peaks from left to right in each graph correspond to zero, one, two, and three trapped holes. When incident light intensity increases, more and more holes are generated. Thus, the possibility of holes being trapped under the LG increases, resulting in higher peaks for more trapped holes. These peaks are clearly separated, indicating that the detector can resolve the number of trapped holes in the time period before recombination takes place. This would lead to the capability of PNR, if the QE could be made closer to unity.

Figure 6(a) shows probabilities of states f_i corresponding to the number of trapped holes i as a function of count rate, namely, hole generation rate R. The theoretical curves (solid curves) are based on Fig. 6(b) under steady-state conditions, $f_i/\tau_i = f_{i-1}R$ and $\Sigma f_i = 1$, where τ_i is the hole lifetime corresponding to i, and 10, 5, and 1 ms are obtained as fitting parameters for $i = 1, 2$, and 3, respectively. Experimental data (solid symbols) and theoretical ones coincide well, suggesting that the hole number can be resolved up to 3 with time resolution smaller than 1 ms.

Since the lifetime of holes is closely related to the hole number resolution, their recombination behavior is further studied. Recombination rate as a function of drain current (not shown here) follows the power law with an exponent of 0.42. This indicates that recombination is not a simple bimolecular process, as opposed to [6]. Contribution of indirect process (e.g., via a recombination center) is a possibility.

It has been shown that a scaled-down SOI MOSFET can be used as a photon detector that directly counts photogenerated holes without multiplication, and features very low dark counts of less than $0.02\,s^{-1}$ at room temperature and low operation voltage of 1 V. Since the detector can clearly resolve the number of photogenerated holes, it could attain PNR if the QE could be raised close to unity.

The authors are indebted to Keisaku Yamada of University of Tsukuba, Toyohiro Chikyo of the National Institute of Materials and Science, Tetsuo Endoh of Tohoku University, and Hideo Yoshino and Shigeru Fujisawa of Semiconductor Leading Edge Technologies, Inc. for their cooperation in the device fabrication.

References

1. W. Becker, A. Bergmann, M. A. Hink, K. König, K. Benndorf, and C. Biskup, Microsc. Res. Tech. **63**, 58 (2004).
2. L. Alaverdian, S. Alaverdian, O. Bilenko, I. Bogdanov, E. Filippova, D. Gavrilov, B. Gorbovitski, M. Gouzman, G. Gudkov, S. Domratchev, O. Kosobokova, N. Lifshitz, S. Luryi, V. Ruskovoloshin, A. Stepoukhovitch, M. Tcherevishnick, G. Tyshko, and V. Gorfinkel, Electrophoresis **23**, 2804 (2002).
3. H. Kosaka, A. Tomita, Y. Nambu, T. Kimura, and K. Nakamura, Electron. Lett. **39**, 1199 (2003).
4. S. Donati, *Photodetectors* (Prentice Hall, 1999).
5. E. J. Gansen, M. A. Rowe, M. B. Greene, D. Rosenberg, T. E. Harvey, M. Y. Su, R. H. Hadfield, S. W. Nam, and R. P. Mirin, Nat. Photon. **1**, 585 (2007).
6. A. Fujiwara, K. Yamazaki, and Y. Takahashi, Appl. Phys. Lett. **80**, 4567 (2002).
7. K. Nishiguchi, Y. Ono, A. Fujiwara, H. Yamaguchi, H. Inokawa, and Y. Takahashi, Appl. Phys. Lett. **90**, 223108 (2007).
8. N. Gisin, G. Ribordy, W. Tittel, and H. Zbinden, Rev. Mod. Phys. **74**, 145 (2002).
9. E. Knill, R. Laflamme, and G. J. Milburn, Nature **409**, 46 (2001).
10. G. A. Morton, H. M. Smith, and H. R. Krall, Appl. Phys. Lett. **13**, 356 (1968).
11. B. E. Kardynał, Z. L. Yuan, and A. J. Shields, Nat. Photon. **2**, 425 (2008).
12. A. E. Lita, A. J. Miller, and S. W. Nam, Opt. Express **16**, 3032 (2008).
13. J. Kim, S. Takeuchi, Y. Yamamoto, and H. Hogue, Appl. Phys. Lett. **74**, 902 (1999).
14. A. Divochiy, F. Marsili, D. Bitauld, A. Gaggero, R. Leoni, F. Mattioli, A. Korneev, V. Seleznev, N. Kaurova, O. Minaeva, G. Goltsman, K. G. Lagoudakis, M. Benkhaoul, F. Lévy, and A. Fiore, Nat. Photon. **2**, 302 (2008).
15. V. Singh, H. Inokawa, T. Endoh, and H. Satoh, Jpn. J. Appl. Phys. **49**, 128002 (2010).
16. W. Du, H. Inokawa, and H. Satoh, in *Extended Abstracts of the 2010 International Conference on Solid State Devices and Materials* (2010), pp. 493–494.
17. T. Ishi, J. Fujikata, K. Makita, T. Baba, and K. Ohashi, Jpn. J. Appl. Phys. **44**, L364 (2005).